


Article

Powder Bed Approach to 3D Printing of Structural Electronic Circuits

Dawid Dembowski * and Marcin Słoma 

Micro- and Nanotechnology Division, Institute of Metrology and Biomedical Engineering,
Faculty of Mechatronics, Warsaw University of Technology, 8 sw. A. Boboli st., 02-525 Warsaw, Poland;
marcin.sloma@pw.edu.pl

* Correspondence: dawid.dembowski.stud@pw.edu.pl

Abstract: The purpose of this study is to research the possibility of producing structural electronics with the powder bed Binder Jetting (BJ) technique. The adaptation of the BJ ZPrinter 450 printer for the deposition of silver nanoparticle inks and the fabrication of conductive paths using commercially available consumables was successfully carried out. The research included testing the influence of different orientations of the printed substrates for the conductive paths and also checking the dependence of the resistance on a number of printed nanoparticle ink layers. First, the measured average resistance value equal to 133.86Ω was reached after 18 printed nanosilver ink layers. The best results have been obtained for 68 printed layers with an average resistance value of 4.64Ω . The effect of the heat-treatment time and multiple sintering approaches of the prepared samples was also examined. The dependence of the sintering time on the resistance of the path turned out to be consistent with that encountered in the literature. Single sintering of the path with 33 nanosilver ink layers gave an average resistance value of 21.11Ω . The same number of layers sintered 3 times during the process after several passes of the printhead gave the lowest resistance value of 1.89Ω . Strength tests of the samples showed that the BJ is not suitable for the application of strain sensor fabrication. Despite this, the results of the study showed that high-efficiency printed electronics are possible to be fabricated using powder bed techniques, and there is a lot of room for future research.

Keywords: additive manufacturing; binder jetting; inkjet; 3D printing; printed electronics; structural electronics; silver nanoparticle ink



Citation: Dembowski, D.; Słoma, M. Powder Bed Approach to 3D Printing of Structural Electronic Circuits.

Electronics **2023**, *12*, 3088. <https://doi.org/10.3390/electronics12143088>

Academic Editors: Tomasz Kozior, Muammel M. Hanon and Łászló Zsidai

Received: 3 June 2023
Revised: 27 June 2023
Accepted: 12 July 2023
Published: 16 July 2023



Copyright: © 2023 by the authors. Licensee MDPI, Basel, Switzerland. This article is an open access article distributed under the terms and conditions of the Creative Commons Attribution (CC BY) license (<https://creativecommons.org/licenses/by/4.0/>).

1. Introduction

Additive manufacturing, commonly known as 3D printing, is a group of techniques where three-dimensional objects are prepared using 3D printers by depositing material layer by layer. Each of them is a cross-section of geometry prepared for manufacturing by computer-aided design (CAD) software, which is then digitally sliced at different heights using computer-aided manufacturing (CAM) software, according to the spatial orientation of the object. Finally, after selecting process parameters, digital data prepared in this way is ready to be converted into machine code and sent to the 3D printer [1,2].

There is a variety of 3D printing technology types that can be divided into categories by material type and method of its deposition [3]. Fused Deposition Modeling (FDM) and Direct Ink Writing (DIW) are based on material extrusion; material jetting is used in Direct Ink Jetting techniques and Aerosol Jet Printing (AJP), whereas Stereolithography (SLA), Digital Light Projection (DLP), Selective Laser Sintering (SLS) and Binder Jetting (BJ) use material curing, melting or binding processes. It should be mentioned that this is only the “tip of the iceberg” and all sorts of modifications or newly developed technologies are emerging each year [1]. Binder Jetting, just like SLS, is an example of huge group of techniques where the building material is in powder form. A precise dose of material is spread by a scraper or roller on the build plate to prepare single layers. Inkjet printheads are

used to apply adhesive material, just like the ink in a conventional inkjet printer, precisely in the areas of the printed element cross-sections. BJ is an efficient, low-temperature 3D printing method where huge amount of composite parts placed through the chamber volume can be prepared in short period of time using large group of materials, both powdered and in the form of ink deposited from the nozzles.

Along with the need to shorten the time between design and production of electronics, the increasing complexity of the devices requiring weight reduction, the rising cost of traditional methods and the growing need for environmental neutrality scientists developed processes and conductive materials for conventional printing methods such as screen printing, flexography, gravure offset lithography or inkjet printing to prepare technology called printed electronics [4]. A step further was to adapt well-known additive manufacturing techniques to produce spatially conductive circuits, which can be prepared on a single 3D printer with reduction of additional processes. Following the achievements of printed electronics, such as developing composite materials with conductive nanoparticles (NPs), nanosheets (NSs) or nanotubes (NTs) interest in the field of 3D printed structural electronics boosted, which resulted in prospective achievements for future studies [1].

Generally, most 3D-printed electronic structures are prepared using several additive manufacturing technologies, which are the easiest to adapt for multi-material printing, where both conductive and insulating material is deposited. Therefore, Fused Deposition Modelling met expectations with the possibility of using polymer composite filaments filled with conductive carbon nanomaterials [5,6] or metal powder-filled composites [7]. Additionally, FDM 3D printers with several nozzles are widely used for printing a few materials in a single process. It is also possible to come across modified FDM technology where fusible metal alloys were used to prepare conductive tracks straight on already printed thermoplastic substrate [8,9]. Using metal NPs as the functional conductive filler in filaments is complicated due to the low possible loading and the need for sintering printed patterns to provide conductivity. However, DIW was successfully adapted for the deposition of silver nanoparticle paste on the thermoplastic substrate, and the paths printed in this way could then be selectively sintered [10]. Preparing 3D printable electrolytes for Li-ion batteries [11] or adapting DIW for additive manufacturing of supercapacitors was also reported [12,13]. Application of Inkjet technology and AJP for structural electronics is also the focus of the researchers' interests due to the possibility of using many other functional nanomaterials. It turned out to be promising to use aerosol jet printing for fabricating microlattices [14] and active RF devices [15]. Inkjet printing was tested mostly for preparing conductive structures using a vast amount of functional nanoparticle inks containing silver NSs [16], silver NPs [17,18], copper NPs [3], carbon nanomaterials [19] or Metallo-Organic Decomposition (MOD) and Catalyst inks [20]. Additive-free aqueous MXene inks were also reported [21]. Inkjet printing is also very popular for the production of biosensors and related bioapplications [22]. Due to their specificity, powder bed 3D printing technologies are difficult to incorporate into structural electronics. Even though it is possible to use conductive powders in SLS technology for preparing electronic devices such as antennas [23] or electrodes [24], the huge barrier is still the impossibility of using multiple materials in one printing process. The situation is extremely different with the binder jetting technology because it allows depositing different functional inks from the printhead even if the powder bed is filled with the same material throughout the process. It causes the BJ technology to become very promising for the fabrication of composite conductive structures.

Despite this, scientists rarely investigate applications of binder jetting in structural electronics. Research focuses mainly on improving the purity and thermal conductivity of the parts printed from metal powder [25] or reducing their porosity [26,27]. A few approaches for BJ in electronic applications are based on preparing conductive structures using carbon-based nanomaterials as functional fillers in binders [28] or the powder itself used for printing [29]. Integrating BJ with AJP and other additional processes to prepare 3D electronic devices was also reported [30]. However, there is a lack of research in the liter-

ature on the use of conductive nanoparticle inks to electrically functionalize printed objects. Therefore, this research, for the first time aims to investigate conductive structures fabricated from BJ technology using silver nanoparticle (AgNP) ink. The influence of substrate printing orientation on the electrical parameters of the printed objects was investigated. We propose a different approach to preparing such structures by depositing conductive ink with an inkjet printhead independent of the one used for the binder. Therefore, it was possible to print several layers of the functional material, which is important in the case of such porous substrates. The influence of the orientation of the printed substrate on silver track resistance was analyzed. The dependence of the resistance of the structures on the number of AgNP ink layers was found. Additionally, an attempt was made to optimize the sintering time as well as test multiple sintering to reach the best possible parameters of the printed paths for applications and development in future studies.

2. Materials and Methods

In this study, high-performance composite powder zp[®]150 (Z Corporation, Burlington, VT, USA) and clear binder solution zb[®]61 (Z Corporation, Burlington, VT, USA) were used for the fabrication of test samples on the automated, mid-range 3D printer ZPrinter 450 (Z Corporation, Burlington, VT, USA) [31]. ZPrinter 450 is a full-color capable Binder Jet 3D printer supporting commercially available thermal inkjet HP11 and HP57 printheads (Hewlett-Packard, Palo Alto, CA, USA). It has a maximum build volume of 203 mm × 254 mm × 203 mm, a building speed of up to 4 layers per minute with layer thicknesses from 0.0875 mm up to 0.125 mm, and a 300 × 450 dpi print resolution.

The material used for the fabrication of conductive paths was commercially available PRELECT TPS303 nanosilver ink (Agfa–Gevaert, Mortsel, Belgium) [32]. The ink is a water-based formulation containing 32 wt% AgNPs with a mean size of about 90 nm. According to the datasheet, ink is suitable for inkjet printing systems. The Z Corporation supplier does not provide the details of the zp[®]150 plaster and polymer-type powder, but a D50 value of 32 μm has been reported previously for this material in the literature [33]. An Auriga 60 (Carl Zeiss, Oberkochen, Germany) scanning electron microscope (SEM) was used for the observations of the morphology of used materials (zp[®]150 powder and TPS303 ink) which are presented in Figure 1.

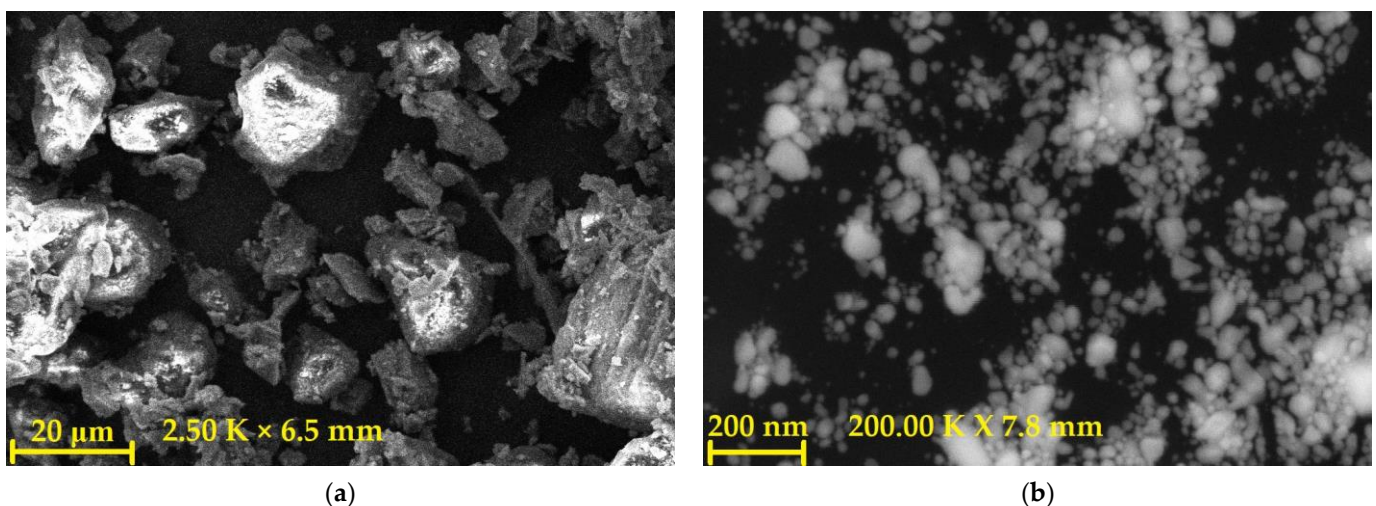


Figure 1. Scanning electron microscope (SEM) images of the materials used for preparing test samples: (a) composite powder zp[®]150; (b) PRELECT TPS303 AgNP ink.

Despite the fact that ZPrinter 450 is equipped with a colorful HP57 thermal inkjet printhead, the printer software limitations do not allow for modification by filling it with different materials. The problem is that the printer needs to print and scan a color alignment pattern after every printhead change, which is impossible with single-color ink. For this

reason, an equivalent HP thermal printing system was used with the HP350 printhead. Such a printing system was also used with thermal heads for the fabrication of printed electronic structures as an alternative to the most popular piezoelectric printing heads used in Dimatix or Pixdro inkjet systems [16,19,20,34].

3D printed samples as substrates for conductive paths were designed in Autodesk Inventor 2023 according to ISO 527-2 standards with modified thickness to match the printing system used. The shape of the conductive tracks to be printed on the samples was designed with contact pads and a narrower path between them. The shape and dimensions of the substrates and the designed conductive paths are presented in Figure 2.

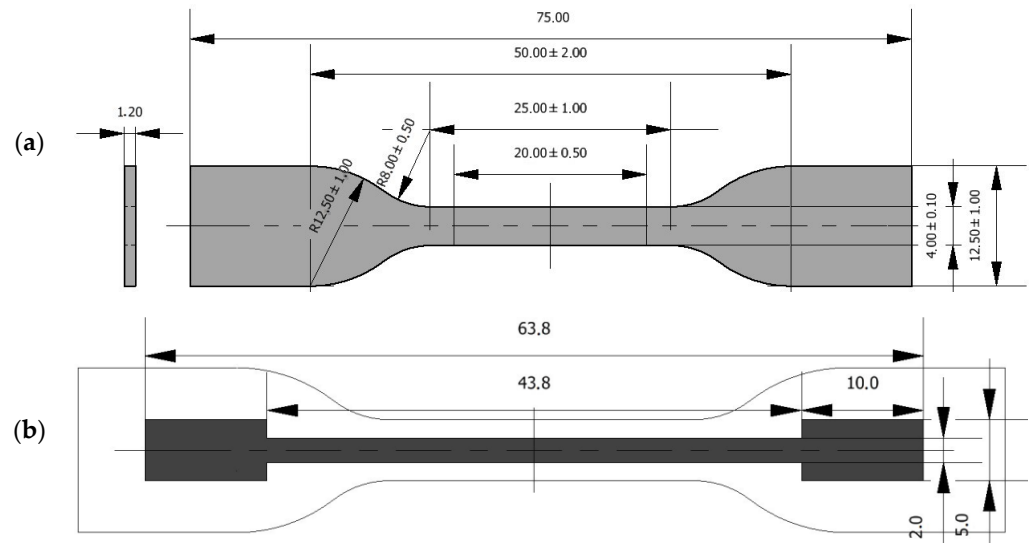


Figure 2. Schematic drawings with dimensions of the printed geometries: (a) 3D printed samples according to ISO 527-2 standard with modified thickness; (b) Geometry of the conductive path projected onto the sample geometry.

The designed sample geometry was exported to the STL file format, sliced and laid out in the workspace using dedicated ZPrint software. Taking into consideration the porosity of the parts produced by BJ and possible differences in resolution depending on the orientation of the parts relative to the printer x -axis, four possible arrangements of the parts were chosen for the test: three series of samples flat on the build plate (parallel, perpendicular and rotated at an angle of 45°) and one series-parallel and horizontally placed. For each chosen orientation, five substrates were made for simplified statistical analysis and observation of the repeatability of results. Most of the process parameters are automatically adapted to the material used, so only the layer thickness has been changed to 0.0875 mm. After the printing process is finished, the 3D printer automatically depowders the printed samples, which need to be brushed and finely depowdered using compressed air.

According to the datasheet, before printing the conductive structures, a test tube with the AgNP ink was placed in an ultrasonic bath for 45 min before filling the printhead [33]. Then, AgNP ink was poured into the previously opened and washed with deionized water HP350 printhead. Precisely closing and sealing the tank was important to avoid uncontrolled ink leakage during the printing process. Printing conductive layers using the HP thermal inkjet system was carried out with the best possible printing quality option chosen with the samples oriented along the axis of the cartridge movement. After every 10 layers were printed, the printhead nozzles were washed with deionized water to prevent clogging. To examine the different orientations of the substrate influencing the electrical properties of the printed path, as a rule of thumb, 30 layers of AgNP ink were initially printed, and such number of layers exhibited sufficient electrical conductivity. For each sample, the sintering process was performed in drying oven for 60 min at 200°C to reach

conductivity. The single load of the samples for simultaneous printing of the paths was 4, which accelerated the process.

Then, after choosing the best substrate for printing conductive paths, the number of subsequent printed layers was selected on the basis of a preferred series guideline based on the E6 series, which has been extended to observe the moment of appearance of conductivity. Therefore, a number of quantities of printed silver layers selected for further research included 10, 15, 18, 22, 33, 47 and 68 layers to observe wide range of the measured resistance and cover the entire decade of needed values. Because of the time-consuming sintering process, additional tests were carried out to check the effect of the sintering time on the conductivity. The influence of repeated sintering of samples on their final resistance was analyzed. For prepared conductive structures, two-point measurements were made using an Escort 3145A (Schmidt Scientific Taiwan Ltd., Taipei City, China) digital multimeter after the sintering process, and Keyence VHX-900 (Keyence Corporation, Osaka, Japan) digital microscope was used for observation of the samples. The Cometech Testing Machine QC-506 (Cometech, Taichung City, Taiwan) was used for tensile tests of the samples.

3. Results and Discussion

3.1. Influence of the Samples Printing Orientation on Electrical Resistance

To evaluate whether the printing orientation of the substrates will affect the electrical parameters of the printed conductive paths, a test series was prepared depending on the orientation angle between the long edge of the sample and the x -axis of the printer: “0f”, “45f” and “90f” for samples aligned flat on the build plate, and “0h” for the series placed horizontally. An example of the arrangement of samples relative to the worktable in the ZPrint software is shown in Figure 3.

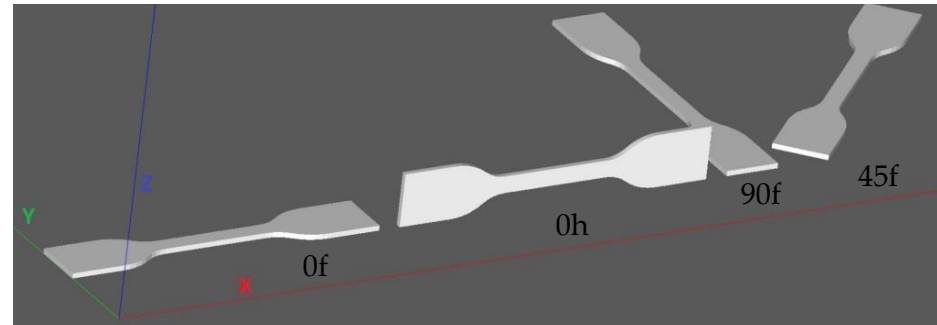


Figure 3. Presentation of the tested printing orientation of the samples, from left: sample “0f”, sample “0h”, sample “90f” and sample “45f”.

As previously mentioned, 30 layers of AgNP ink were deposited on the differently oriented sample and thermally sintered. The example photographs of prepared samples are presented in Figure 4.

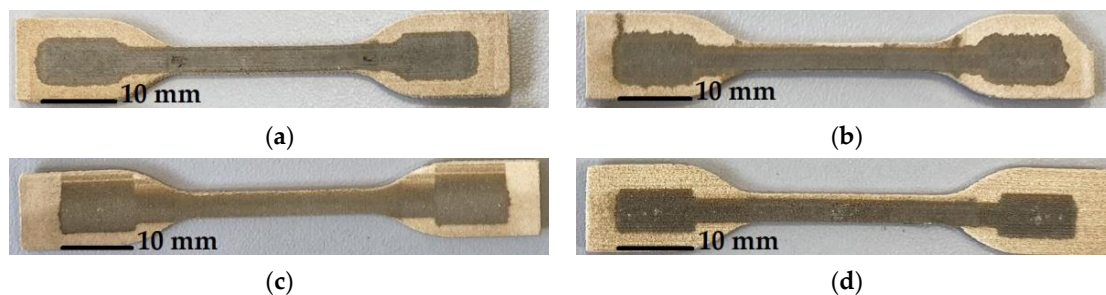


Figure 4. Representative samples printed in different orientations: (a) sample “0f”; (b) sample “45f”; (c) sample “90f”; (d) sample “0h”. Differences in line color are only due to the camera limitations.

Resistance measurements have shown that only 2 series of samples provide current conductivity. The measured values are presented in Table 1.

Table 1. Resistance values of the samples printed in different orientations. (“x” denotes samples that exhibited no electrical conductivity).

Sample Series Symbol	Measured Resistance [Ω]
0f	40.42 ± 2.20
45f	70.64 ± 21.08
90f	x
0h	x

The results of the study clearly showed that substrates from the “0f” series should be selected for further testing. These samples had the best conductivity along the entire length of the sample and the best repeatability, which was not so noticeable for “45f” samples despite the measured conductivity. Additionally, “0f” substrates were less fragile and less pliable as a result of ink soaking after AgNP ink printing. Series “90f” and “0h” exhibited no conductivity at all, but they could be measured in certain parts of the paths. Visually the samples did not differ much from each other, which is visible in Figure 4. The problem with sample conductivities was identified by microscopy observation of the printed paths. Images taken by optical microscope are presented in Figure 5. In the pictures, it can be seen that the paths on “90f” (Figure 5c) and “0h” (Figure 5d) samples are heavily cracked, which influenced the continuity of the paths and thus the electrical connection could not be measured. The direction of the cracks is consistent with the substrate orientation during the printing process. As can be seen, cracks on the “90f” samples are perpendicular to the expected direction of electrical current flow through the path, causing the discontinuities. The weakly bonded interlayer space and stress in the samples due to sintering and cooling caused cracks in these areas. Moreover, the smaller dimension of the path in this direction caused more intense cracking of the silver layer compared to the path printed along the sample. The “90f” and “45f” samples were more fragile than others and could be easily damaged in the hands. Despite the fact that “0h” substrates were less prone to transverse cracking, low print resolution in the z-axis of printed layers promoted longitudinal shallow cracks on the silver paths as well (Figure 5d). Additionally, the surface of the paths was very heterogeneous due to the surface irregularities associated with the low print resolution in this direction. The surface of the deposited ink was arranged in a series of regular, parallel and narrow metallic structures that could be easily damaged during the sintering, resulting in a break in the conductive paths. In addition, these samples showed the greatest deformation resulting from the sintering process. Sample “0f” shows the most uniform surface structure of the path (Figure 5a).

3.2. Influence of the Printed Conductive Layers Number on Resistance

In the next experiments, only “0f” series samples of the printed substrates were chosen to check the relationship between resistance and the number of printed conductive layers. To investigate this, the extended E6 preferred series set was used to select the number of subsequent passes. This allowed us to observe a wide spectrum of resistance values, from weakly conductive samples to the better ones. Figure 6 shows all the printed samples used for this study.

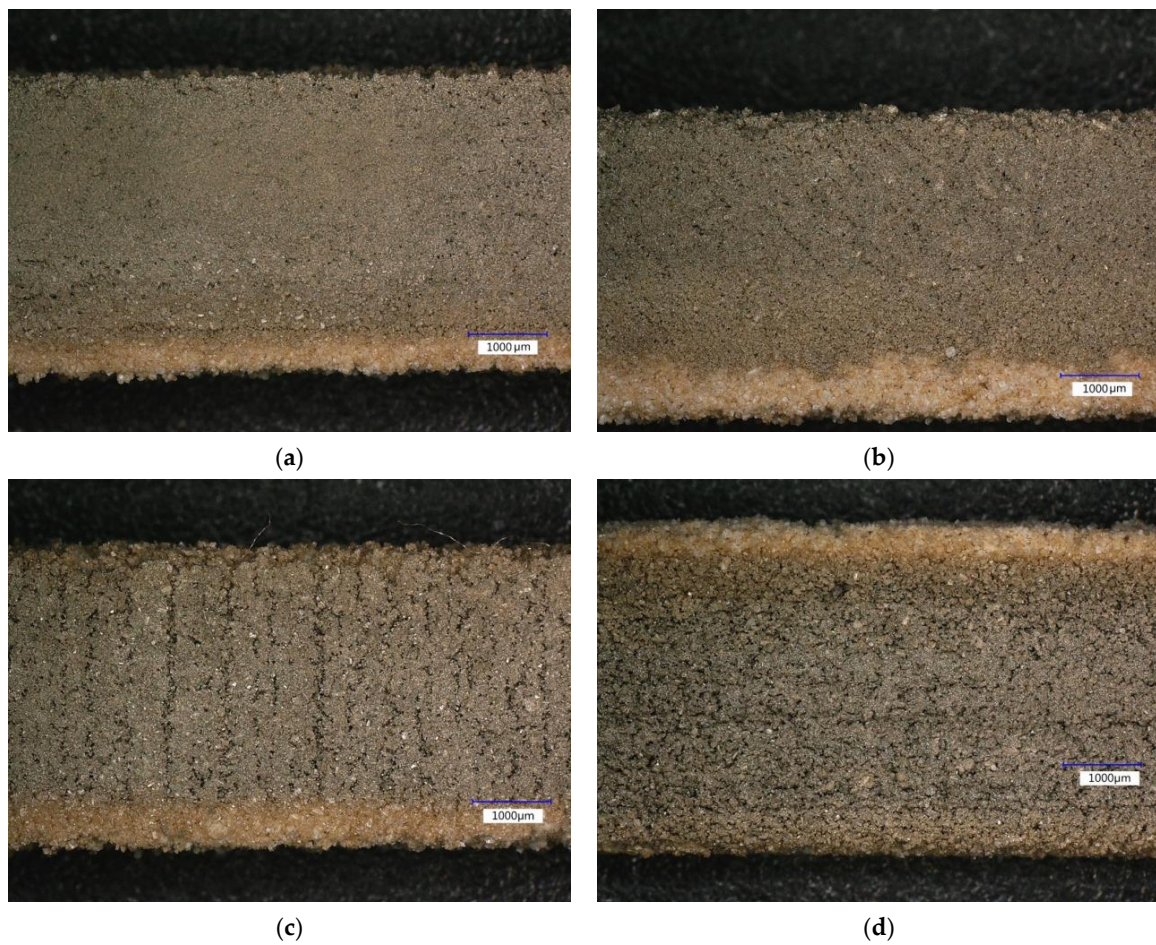


Figure 5. Images of the paths printed from AgNP ink printed on the substrates prepared with different orientations in BJ printing process: (a) sample "0f"; (b) sample "45f"; (c) sample "90f"; (d) sample "0h".

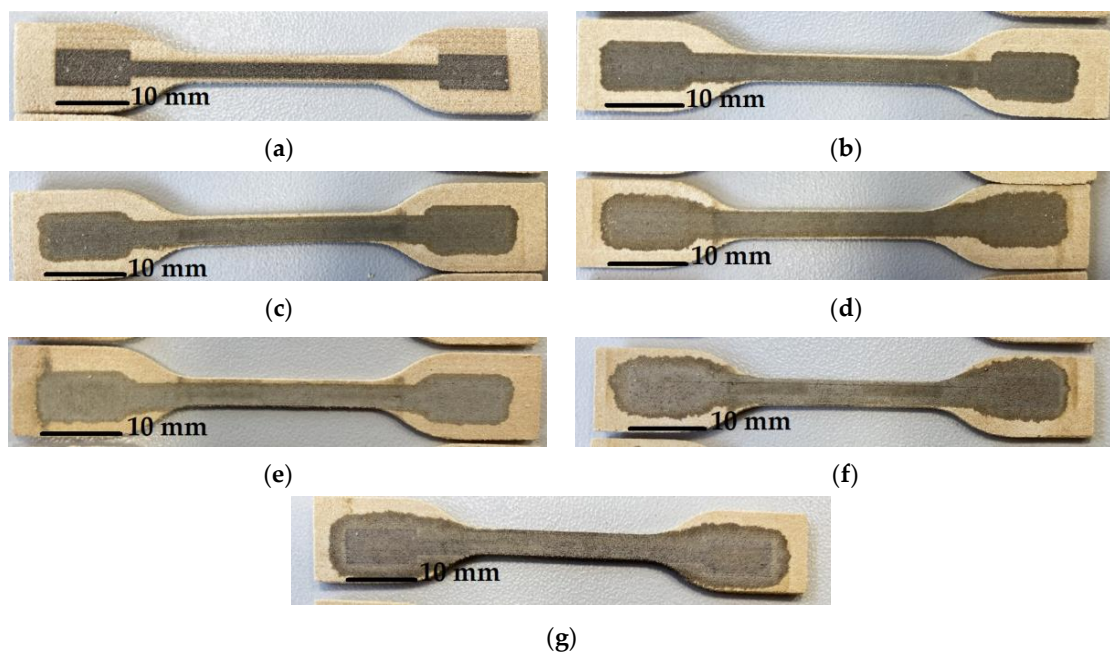


Figure 6. Images of the representative samples with different number of printed AgNP ink layers: (a) 10 layers; (b) 15 layers; (c) 18 layers; (d) 22 layers; (e) 33 layers; (f) 47 layers; (g) 68 layers.

The results obtained from the resistance measurements of the samples are presented in Figure 7.

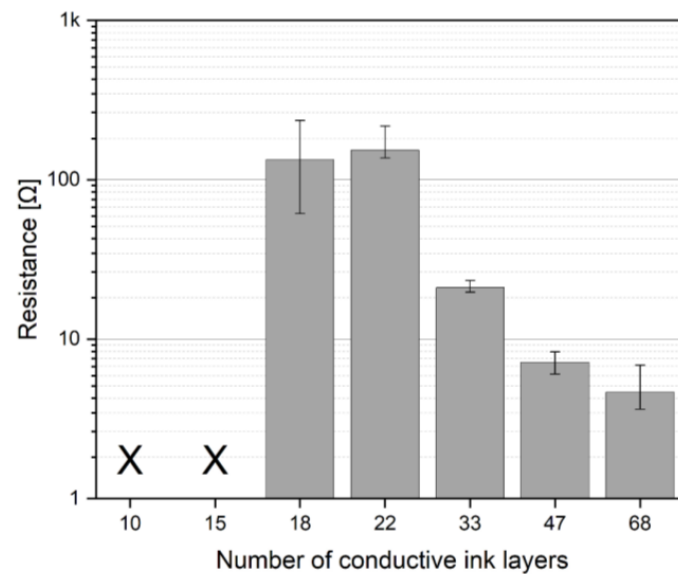


Figure 7. Resistance values depending on the number of printed AgNP ink layers. “x” denotes samples that exhibited no electrical conductivity.

It is apparent that samples did not conduct after printing 10 and 15 ink layers. This is due to too little deposited ink, which easily soaked into the shallow layers of the porous substrate. Silver nanoparticles penetrated the pores, resulting in composite powder-ink structures, so that a small amount of them remains on the surface to create a conductive path. After printing 18 layers of the AgNP ink, the resistance was first measured with an average value comparable to the subsequently printed path of 22 layers. However, the deviation of results for this series of samples (18 layers) was the largest among those examined. This can be related to the very heterogeneous silver path structure for a small number of printed layers, which results in low repeatability of the obtained resistance values. For the same reason, measured resistances were not converted to resistivities, which is a common practice in the literature referring to structural electronics. The conductive path is a composite of the bonded powder and sintered nanoparticle ink, which is a heterogeneous material with an unknown exact thickness of the conductive part of the path. Generally, printed path resistance values decreased with the rising number of printed AgNP ink layers to reach the minimum value for 68 printed layers. Despite achieving satisfactory resistance results, the decreasing deviation began to increase in the number of layers above 33. As can be seen in Figure 6, with the rising number of layers, ink absorption to the sides increased on the surface of the substrate. A representative example of the ink-soaked sample after 68 printhead passes is presented in Figure 8. The rising number of ink layers causes a situation in which the porous substrate is no longer able to absorb more nanosilver ink that seeps through the entire thickness of the sample (Figure 8b,c). The pictures clearly show the softening of the sample and the soaking of the ink to the sides (Figure 8a). As a result, conductive paths printed more times did not retain their dimensions consistent with those designed. However, this did not affect resistance measurement but caused increased dispersion of the results between samples with a huge number of printed ink layers.

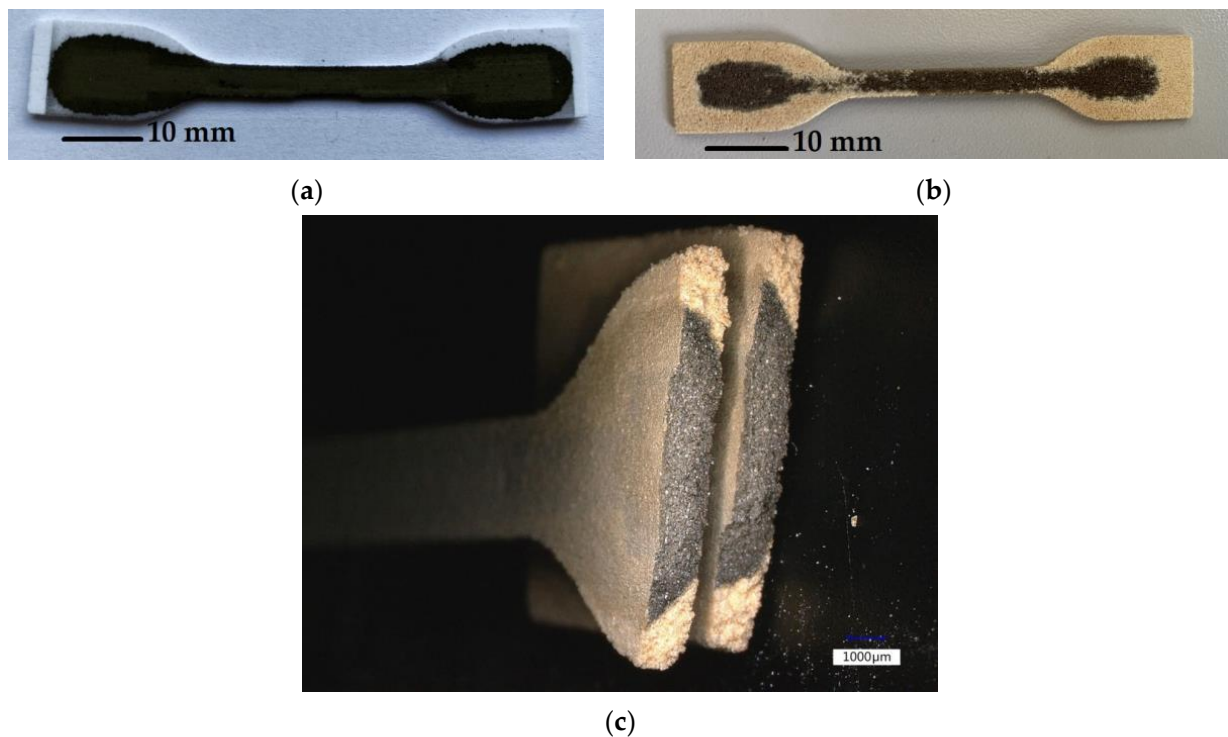


Figure 8. Images of ink-soaked samples: (a) 68 layers of AgNP ink printed on the substrate and visible softening and soaking of the sample before sintering; (b) Same sample after sintering presented on the back side to show the ink penetration through the sample; (c) Cross-section of the sample.

3.3. Influence of the Sintering Time on Resistance and Samples Physical Parameters

To investigate the influence of the sintering time on the path resistance, the series with the lowest resistance was chosen. Here, 60-min sintering is recommended by the manufacturer to reach the optimal conductivity of the ink, but that refers to printing on a glass substrate [33]. To check the effect of sintering time on the electrical parameters, the samples with 68 layers of AgNP ink were sintered for 3 different periods of time, and then resistance measurement was carried out. The results of this investigation are presented in Figure 9.

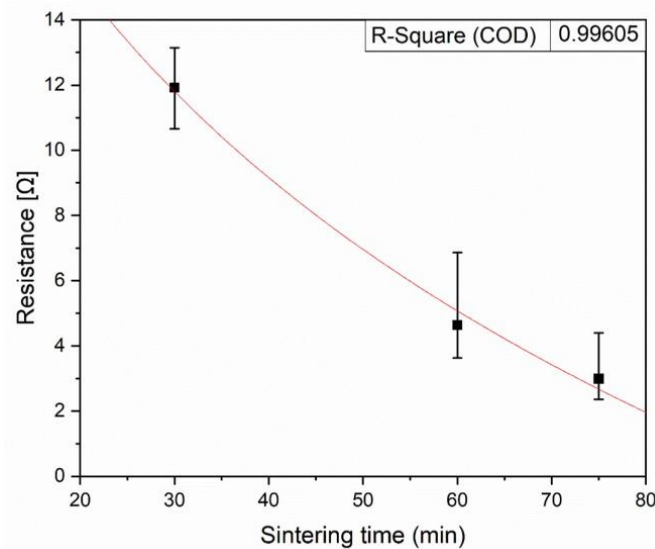


Figure 9. Plot of dependence of path resistance on sintering time.

It has been observed that the increasing sintering time allowed the resistance to decrease. The nature of the resistance change as a function of sintering time can be approximated with high probability by a logarithmic function. The drop in resistance was less exponential between 60 and 75 min of sintering, so we can predict that further increasing the sintering time would not significantly affect the resistance. Similar relations between sintering time and resistance of the inkjet-printed structures from metal nanoparticle inks were reported in the literature [35–37]. To melt and form a continuous path, AgNPs require the same energy to be delivered in the sintering process in the whole volume of the conductive paths, both for the particles on the surface and particles that have soaked deeper into the porous substrate. Therefore, the sintering time cannot be too short due to the need to melt all the deposited nanoparticles. On the other hand, a longer sintering time significantly weakens the mechanical properties of the composite substrate. The longer the substrate was sintered, the more brittle it became. It can be seen visually in Figure 10, where the silver path became lighter and the substrate darkened due to the temperature degradation of the organic binder. A similar effect is expected in the case of adjusting the sintering temperature. Despite better sample conductivity after 75 min of sintering due to the strong brittleness of the substrates, 60 min of sintering should be considered optimal for this type of substrate composite material.

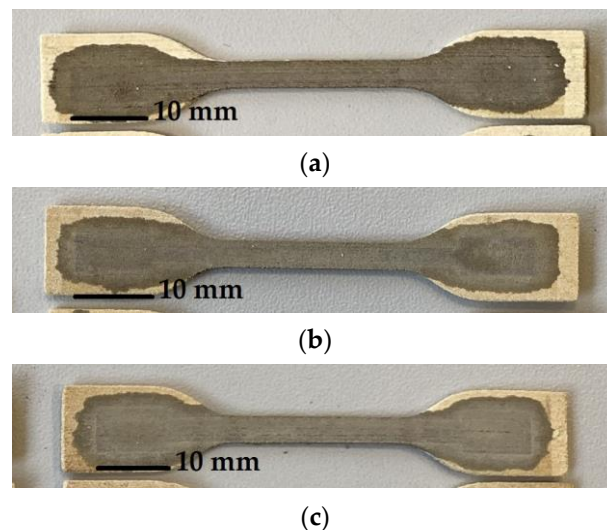


Figure 10. Representative samples with 68 layers of printed AgNP ink after different sintering times: (a) 30 min; (b) 60 min; (c) 75 min.

3.4. Influence of the Multiple Printing and Sintering on Resistance

After performing an optimal sintering time test, there was an idea to try to further reduce the resistance of the paths as a result of duplicating the sintering process after several printed nanosilver ink layers. However, using sintering times that resulted in the best resistance values would be too time-consuming for sintering several times. It would cause the process to be poorly optimized, and samples would be too fragile. For these reasons, 30-min time for each of the sintering processes was chosen. Such a multiple printing and sintering approach was performed until the number of printed ink layers was achieved according to the chosen value or the extended E6 series. To reach the optimal time of the process, samples with 33 layers of AgNP ink were chosen for the study. Additionally, this series, as presented in Figure 7, showed the smallest dispersion in the resistance values. The test was divided into three groups, where samples were sintered once (after 33 printed layers), twice (after 16 and 33 printed layers) and three times (after 11, 22 and 33 printed layers). Representatives of such printed samples are presented in Figure 11.

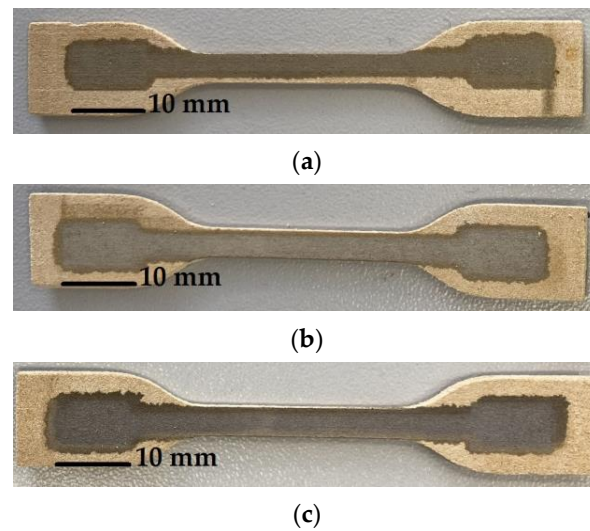


Figure 11. Images of the representative samples sintered multiple times with 33 layers of the nanosilver ink: (a) sample after single sintering; (b) sample after dual sintering; (c) sample after triple sintering.

As can be seen, samples are almost identical visually except for the color of the path, which became more silver-metallic with the rising number of sintering cycles. Larger differences are visible in microscopic images of samples in Figure 12. The results from resistance measurement of prepared multiple-sintered samples are presented in Table 2.

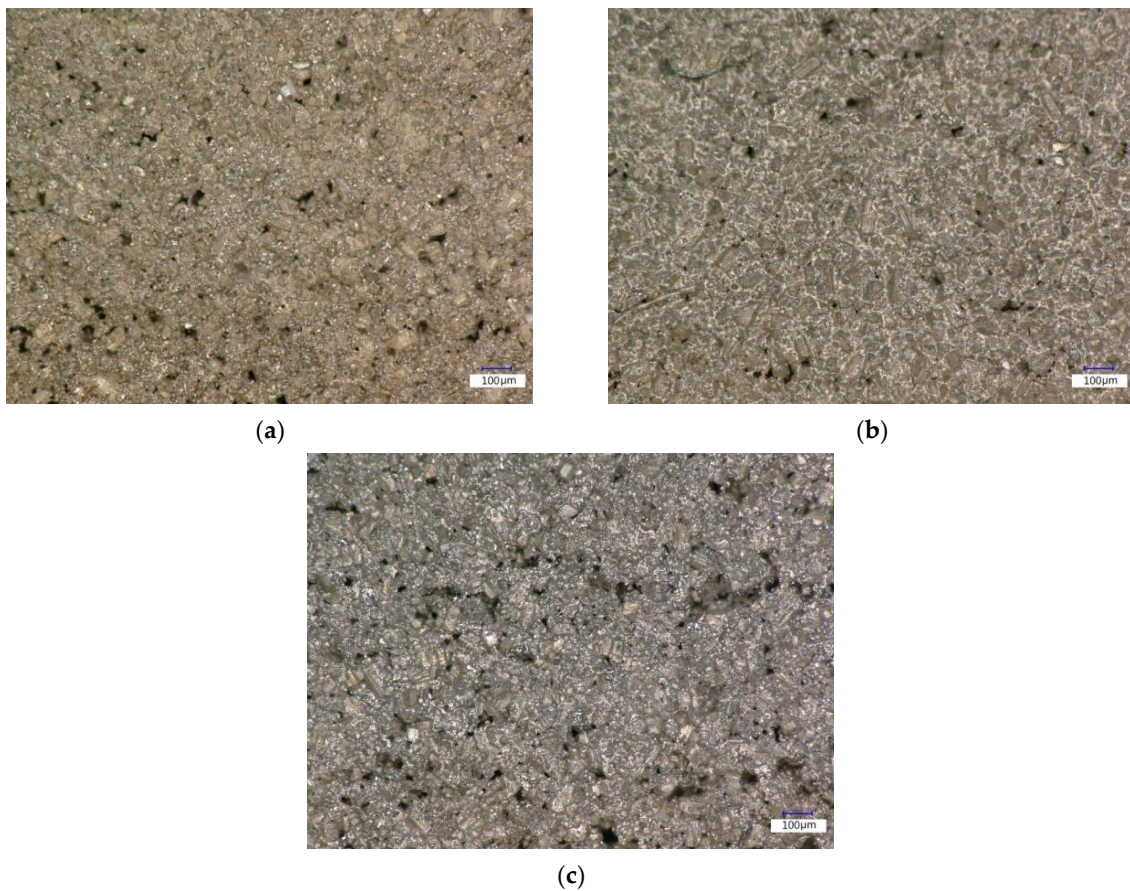


Figure 12. Micrographs of the printed and sintered paths: (a) single sintering; (b) dual sintering; (c) triple sintering.

Table 2. Measured resistance values depending on the number of sintering processes.

Number of Sintering Processes While Preparation	Total Sintering Time [min]	Resistance [Ω]
1	30	34.01 ± 0.99
2	60	2.90 ± 0.27
3	90	1.89 ± 0.48

The above results clearly show that after multiple sinterings of the samples, resistance strongly decreased, obtaining the best conductivity among all samples made in this study. The reason is that after several layers of AgNP ink were sintered, the next one was printed on a changed substrate in the form of a composite of bonded powder and sintered AgNPs, which was less porous and afterward resulted in much denser infiltration of silver ink. Differences between once, twice and three times sintered nanosilver ink paths are visible in Figure 12. The structure of the printed plates is much more homogeneous and uniform for double and triple sintering. For both dual and triple sintering, there are more silver areas visible (Figure 12b,c). However, such approach to the sintering process causes difficulties related to multiple cycles of printing and sintering, disturbing the integrity of the samples and greatly modifying a single-step process of 3D printing.

3.5. Strength Tests of the Samples with the Resistance Measurement of the Paths

Selected samples from each prepared series, corresponding to the number of printed layers of AgNP ink, were subjected to static tensile tests. Additionally, this was combined with the simultaneous measurement of the resistance of representative samples to investigate the potential applications of the prepared conductive structures as resistive strain sensors. To achieve this, dog-bone-shaped samples were placed in the testing machine grips with additional dielectric separators. Probes from a multimeter were attached to the contact fields of the conductive paths to enable resistance measurement at regular time intervals throughout the entire duration of the test until sample failure. Not all prepared samples were suitable for testing due to their fragility, which made them very easily broken when locked in the grips. The stress-strain curve for all samples and the relative resistance changes as a function of applied force for representative samples are presented in Figure 13.

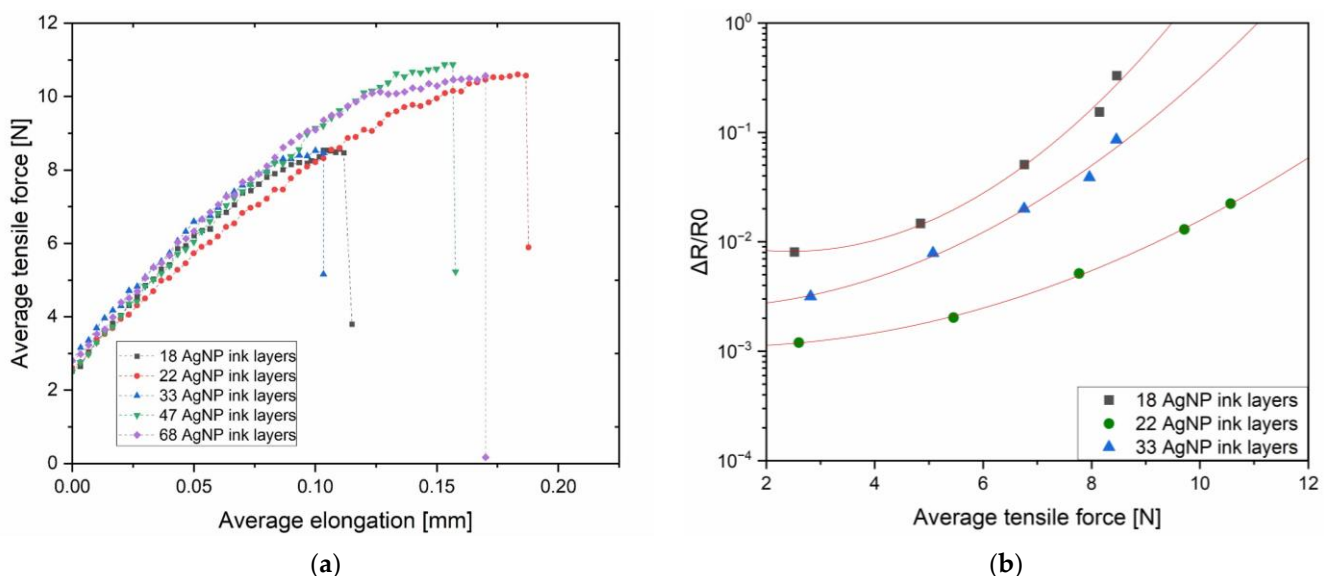


Figure 13. Results of the static tensile test with resistance measurements presented in the plots: (a) force versus elongation diagram; (b) plot of dependence of relative resistance change on applied tensile force.

Analyzing the force versus elongation curve, it is evident that all samples exhibit brittle fracture. The curve progression for each series up to the point of rupture is similar, while the maximum elongation values of the samples do not show any dependency on the number of printed AgNP ink layers on the substrate. The tested samples are very weak and brittle, as indicated by the low values of maximum tensile stress before failure. Therefore, the amount of nanosilver ink applied on the BJ-printed substrates does not significantly affect the mechanical properties of the samples. The low mechanical properties of the samples were influenced by their high-temperature sintering, which was solely necessary to achieve the conductivity of the applied AgNP ink. Unfortunately, the strong impact of high temperatures on the substrate proved to be an unintended side effect.

Moving on to the analysis of the nature of relative resistance change as a function of applied force, we can observe that the characteristics of selected samples can be approximated by square functions. Such representative samples were chosen because the relative resistance change is more noticeable for samples with higher resistance. However, the range of this change is still very low, and the rapid break of the sample limits the measurable force to very small values. The application of BJ-printed conductive structures as strain sensors is possible but problematic due to the narrow measurement range of the tensile force values. Nevertheless, this approach could be incorporated into the reliability and quick fatigue damage test of such 3D printed elements with the presented inkjet-printed sensors.

4. Conclusions

In this study, conductive 3D printed structures were fabricated using binder jetting technology which was rarely investigated in the literature. During the research, the influence of several parameters of the element fabrication process on the resistance of the printed paths were evaluated, such as the direction of the substrate printing, number of printed conductive layers, heat-treatment time and number of the sintering processes during sample preparation. The study shows that the best electrical parameters can be achieved when the substrate printing direction is consistent with the conductive ink deposition direction, i.e., the binder printhead axis is consistent with the ink printhead axis. The sintering process, which is necessary to ensure the electrical conductivity of the AgNP ink layers, gave the best results after extending the time of the process beyond what was recommended by the manufacturer. This, on the other hand, has negative impact on the substrate mechanical properties. Therefore, for multiple sintering tests, the time of the process has been shortened to compromise good electrical parameters with the lowest possible thermal impact on the substrate, and it gave the expected results in the form of the best conductivity among all the samples made for this research. Strength tests of the samples have shown that conductive structures with AgNPs prepared in BJ technology are not very efficient as strain sensors. Nevertheless, an optimized number of printed AgNP ink layers gives the possibility of printing conductive paths with satisfactory electrical parameters that could be used for additive manufacturing of spatial integrated electronic circuits. Future research on this topic could focus on exploring different selective sintering methods, including chemical or photonic techniques, as well as infiltrating samples with waxes, polymers or salts before printing conductive paths. Noteworthy issues for future studies are also the physical parameters of the internal structure of the printed elements, such as the density and volume fraction of all composite components or intermolecular spaces. To reach the best possible approach to structural electronics using BJ technology, it should be adapted for printing not only plain conductive structures but also buried or interlayered paths, which seems possible with some modifications and integrations of BJ with other 3D printing techniques.

Author Contributions: Conceptualization, D.D. and M.S.; methodology, D.D. and M.S.; validation, D.D. and M.S.; formal analysis, M.S.; investigation, D.D.; writing—original draft preparation, D.D.; writing—review and editing, M.S.; visualization, D.D.; supervision, M.S.; project administration, M.S.; funding acquisition, M.S. All authors have read and agreed to the published version of the manuscript.

Funding: This research was funded by the Foundation for Polish Science (FNP) under Grant Number First TEAM/2016-1/7, co-financed by the European Union under the European Regional Development Fund, and Warsaw University of Technology under “3D printed Autonomous Sensors—3D-ASy” grant, agreement no. 504/04765/1142/43.022201.

Data Availability Statement: The data presented in this study are available on request from the corresponding author.

Acknowledgments: This work was supported by the Institute of Metrology and Biomedical Engineering, Warsaw University of Technology, Faculty of Mechatronics. The authors would like to gratefully acknowledge VIGO PHOTONICS S.A. for hardware support.

Conflicts of Interest: The authors declare no conflict of interest.

References

1. Słoma, M. 3D Printed Electronics with Nanomaterials. *Nanoscale* **2023**, *15*, 5623–5648. [[CrossRef](#)] [[PubMed](#)]
2. Dembek, K.; Podsiadły, B.; Słoma, M. Influence of Process Parameters on the Resistivity of 3D Printed Electrically Conductive Structures. *Micromachines* **2022**, *13*, 1203. [[CrossRef](#)] [[PubMed](#)]
3. Lee, D.K.; Sin, K.S.; Shin, C.; Kim, J.H.; Hwang, K.T.; Kim, U.S.; Nahm, S.; Han, K.S. Fabrication of 3D Structure with Heterogeneous Compositions Using Inkjet Printing Process. *Mater. Today Commun.* **2023**, *35*, 105753. [[CrossRef](#)]
4. Nie, X.; Wang, H.; Zou, J. Inkjet Printing of Silver Citrate Conductive Ink on PET Substrate. *Appl. Surf. Sci.* **2012**, *261*, 554–560. [[CrossRef](#)]
5. Podsiadły, B.; Matuszewski, P.; Skalski, A.; Słoma, M. Carbon Nanotube-Based Composite Filaments for 3d Printing of Structural and Conductive Elements. *Appl. Sci.* **2021**, *11*, 1272. [[CrossRef](#)]
6. Dorigato, A.; Moretti, V.; Dul, S.; Unterberger, S.H.; Pegoretti, A. Electrically Conductive Nanocomposites for Fused Deposition Modelling. *Synth. Met.* **2017**, *226*, 7–14. [[CrossRef](#)]
7. Podsiadły, B.; Skalski, A.; Wałpuski, B.; Słoma, M. Heterophase Materials for Fused Filament Fabrication of Structural Electronics. *J. Mater. Sci. Mater. Electron.* **2019**, *30*, 1236–1245. [[CrossRef](#)]
8. Podsiadły, B.; Bežgan, L.; Słoma, M. 3D Printed Electronic Circuits from Fusible Alloys. *Electronics* **2022**, *11*, 3829. [[CrossRef](#)]
9. Zhang, P.; Yu, Y.; Chen, B.; Wang, W.; Wei, S.; Rao, W.; Wang, Q. Fast Fabrication of Double-Layer Printed Circuits Using Bismuth-Based Low-Melting Alloy Beads. *J. Mater. Chem. C Mater.* **2020**, *8*, 8028–8035. [[CrossRef](#)]
10. Wałpuski, B.; Słoma, M. Additive Manufacturing of Electronics from Silver Nanopowders Sintered on 3D Printed Low-Temperature Substrates. *Adv. Eng. Mater.* **2021**, *23*, 2001085. [[CrossRef](#)]
11. Blake, A.J.; Kohlmeyer, R.R.; Hardin, J.O.; Carmona, E.A.; Maruyama, B.; Berrigan, J.D.; Huang, H.; Durstock, M.F. 3D Printable Ceramic–Polymer Electrolytes for Flexible High-Performance Li-Ion Batteries with Enhanced Thermal Stability. *Adv. Energy Mater.* **2017**, *7*, 1602920. [[CrossRef](#)]
12. Rocha, V.G.; García-Tuñón, E.; Botas, C.; Markoulidis, F.; Feilden, E.; D’Elia, E.; Ni, N.; Shaffer, M.; Saiz, E. Multimaterial 3D Printing of Graphene-Based Electrodes for Electrochemical Energy Storage Using Thermoresponsive Inks. *ACS Appl. Mater. Interfaces* **2017**, *9*, 37136–37145. [[CrossRef](#)] [[PubMed](#)]
13. Shen, K.; Ding, J.; Yang, S. 3D Printing Quasi-Solid-State Asymmetric Micro-Supercapacitors with Ultrahigh Areal Energy Density. *Adv. Energy Mater.* **2018**, *8*, 1800408. [[CrossRef](#)]
14. Saleh, M.S.; Hu, C.; Panat, R. Three-Dimensional Microarchitected Materials and Devices Using Nanoparticle Assembly by Pointwise Spatial Printing. *Sci. Adv.* **2017**, *3*, e1601986. [[CrossRef](#)] [[PubMed](#)]
15. Jones, C.S.; Lu, X.; Renn, M.; Stroder, M.; Shih, W.S. Aerosol-Jet-Printed, High-Speed, Flexible Thin-Film Transistor Made Using Single-Walled Carbon Nanotube Solution. *Microelectron. Eng.* **2010**, *87*, 434–437. [[CrossRef](#)]
16. Kelly, A.G.; O’Reilly, J.; Gabbett, C.; Szydłowska, B.; O’Suilleabhain, D.; Khan, U.; Maughan, J.; Carey, T.; Sheil, S.; Stamenov, P.; et al. Highly Conductive Networks of Silver Nanosheets. *Small* **2022**, *18*, 2105996. [[CrossRef](#)]
17. Schuppert, A.; Thielen, M.; Reinhold, I.; Schmidt, W.A.; Schoeller, F. Ink Jet Printing of Conductive Silver Tracks from Nanoparticle Inks on Mesoporous Substrates. In Proceedings of the 27th International Conference on Digital Printing Technologies, NIP27 and 7th International Conference on Digital Fabrication 2011, Minneapolis, MN, USA, 2–6 October 2011.
18. Nogi, M.; Koga, H.; Suganuma, K. Highly Conductive Ink-Jet-Printed Lines. In *Organic Electronics Materials and Devices*; Springer: Tokyo, Japan, 2015; pp. 117–137, ISBN 9784431556541.
19. Wang, S.; Liu, N.; Tao, J.; Yang, C.; Liu, W.; Shi, Y.; Wang, Y.; Su, J.; Li, L.; Gao, Y. Inkjet Printing of Conductive Patterns and Supercapacitors Using a Multi-Walled Carbon Nanotube/Ag Nanoparticle Based Ink. *J. Mater. Chem. A Mater.* **2015**, *3*, 2407–2413. [[CrossRef](#)]
20. Chen, S.-P.; Chiu, H.-L.; Wang, P.-H.; Liao, Y.-C. Inkjet Printed Conductive Tracks for Printed Electronics. *ECS J. Solid State Sci. Technol.* **2015**, *4*, P3026–P3033. [[CrossRef](#)]
21. Uzun, S.; Schelling, M.; Hantanasirisakul, K.; Mathis, T.S.; Askeland, R.; Dion, G.; Gogotsi, Y. Additive-Free Aqueous MXene Inks for Thermal Inkjet Printing on Textiles. *Small* **2021**, *17*, 2006376. [[CrossRef](#)]

22. Hussain, A.; Abbas, N.; Ali, A. Inkjet Printing: A Viable Technology for Biosensor Fabrication. *Chemosensors* **2022**, *10*, 103. [CrossRef]
23. Huang, G.L.; Zhou, S.G.; Chio, T.H.; Yeo, T.S. Fabrication of a High-Efficiency Waveguide Antenna Array via Direct Metal Laser Sintering. *IEEE Antennas Wirel. Propag. Lett.* **2015**, *15*, 622–625. [CrossRef]
24. Zhou, Z.; Wu, X.F. Graphene-Beaded Carbon Nanofibers for Use in Supercapacitor Electrodes: Synthesis and Electrochemical Characterization. *J. Power Sources* **2013**, *222*, 410–416. [CrossRef]
25. Bai, Y.; Williams, C.B. An Exploration of Binder Jetting of Copper. *Rapid Prototyp. J.* **2015**, *21*, 177–185. [CrossRef]
26. Bai, Y.; Williams, C.B. Binder Jetting Additive Manufacturing with a Particle-Free Metal Ink as a Binder Precursor. *Mater. Des.* **2018**, *147*, 146–156. [CrossRef]
27. Bai, Y.; Williams, C.B. The Effect of Inkjetted Nanoparticles on Metal Part Properties in Binder Jetting Additive Manufacturing. *Nanotechnology* **2018**, *29*, 395706. [CrossRef] [PubMed]
28. Shen, X.; Chu, M.; Hariri, F.; Vedula, G.; Naguib, H.E. Binder Jetting Fabrication of Highly Flexible and Electrically Conductive Graphene/PVOH Composites. *Addit. Manuf.* **2020**, *36*, 101565. [CrossRef]
29. Azhari, A.; Marzbanrad, E.; Yilman, D.; Toyserkani, E.; Pope, M.A. Binder-Jet Powder-Bed Additive Manufacturing (3D Printing) of Thick Graphene-Based Electrodes. *Carbon* **2017**, *119*, 257–266. [CrossRef]
30. Hoerber, J.; Glassroeder, J.; Pfeffer, M.; Schilp, J.; Zaeh, M.; Franke, J. Approaches for Additive Manufacturing of 3D Electronic Applications. In *Proceedings of the Procedia CIRP*; Elsevier B.V.: Amsterdam, The Netherlands, 2014; Volume 17, pp. 806–811.
31. ZPrinter®450 Hardware Manual. Available online: <https://www.manualslib.com/manual/1216183/Zcorporation-Zprinter-450.html> (accessed on 29 May 2023).
32. Technical Data Sheet PRELECT TPS303. Available online: www.agfa.com/conductivematerials (accessed on 29 May 2023).
33. Shakor, P.; Nejadi, S.; Paul, G.; Sanjayan, J. A Novel Methodology of Powder-Based Cementitious Materials in 3D Inkjet Printing for Construction Applications. In *Proceedings of the Sixth International Conference on Durability of Concrete Structures (ICDCS 2018)*, Leeds, UK, 18–20 July 2018.
34. Bidoki, S.M.; Lewis, D.M.; Clark, M.; Vakorov, A.; Millner, P.A.; McGorman, D. Ink-Jet Fabrication of Electronic Components. *J. Micromech. Microeng.* **2007**, *17*, 967–974. [CrossRef]
35. Niittynen, J.; Abbel, R.; Mäntysalo, M.; Perelaer, J.; Schubert, U.S.; Lupo, D. Alternative Sintering Methods Compared to Conventional Thermal Sintering for Inkjet Printed Silver Nanoparticle Ink. *Thin Solid Films* **2014**, *556*, 452–459. [CrossRef]
36. Halonen, E.; Viiru, T.; Östman, K.; Cabezas, A.L.; Mantysalo, M. Oven Sintering Process Optimization for Inkjet-Printed Ag Nanoparticle Ink. *IEEE Trans. Compon. Packag. Manuf. Technol.* **2013**, *3*, 350–356. [CrossRef]
37. Kang, J.S.; Kim, H.S.; Ryu, J.; Thomas Hahn, H.; Jang, S.; Joung, J.W. Inkjet Printed Electronics Using Copper Nanoparticle Ink. *J. Mater. Sci. Mater. Electron.* **2010**, *21*, 1213–1220. [CrossRef]

Disclaimer/Publisher’s Note: The statements, opinions and data contained in all publications are solely those of the individual author(s) and contributor(s) and not of MDPI and/or the editor(s). MDPI and/or the editor(s) disclaim responsibility for any injury to people or property resulting from any ideas, methods, instructions or products referred to in the content.